Journal of Superconductivity and Novel Magnetism (2018) 31:3167–3174
https://doi.org/10.1007/s10948-017-4551-1

ORIGINAL PAPER

The Effect of Using Different Y_2O_3 Layers on the Activation Energy and Irreversibility Line of MPMG YBCO Bulk at 1050 °C Growth Temperature

Sedat Kurnaz[1] · **Bakiye Çakır**[1,2] · **Alev Aydıner**[1]

Received: 4 December 2017 / Accepted: 23 December 2017 / Published online: 15 February 2018

Abstract

In this study, three kinds of YBCO samples which are named Y1, Y2 and Y3 were fabricated by a melt–powder–melt–growth (MPMG) method. The Y1 sample was placed into a platinum (Pt) crucible without Y_2O_3, the Y2 sample was located on a Al_2O_3 crucible with a freely poured Y_2O_3 powder and the Y3 sample was located on a Al_2O_3 crucible with a 1-mm-thick buffer layer of Y_2O_3. YBCO samples were investigated by magnetoresistivity (ρ–T) measurements in dc magnetic fields (parallel to the c-axis) up to 5 T. The effect of the Y_2O_3 layer on the activation energy and irreversible flux of the samples was studied. The activation energies (U) were determined using the Arrhenius activation energy law from ρ–T. The power law relationship for U with $H^{-\alpha}$ was investigated. α was calculated to find out which defects were dominant in the samples. Irreversibility fields (H_{irr}) and upper critical fields (H_{c2}) were obtained using 10 and 90% criteria of the normal-state resistivity value from ρ–T curves. Irreversibility lines (ILs) were estimated from the equation $H_{irr} \sim (1 - T_{irr}(H)/T_{irr}(0))^n$. The fitting results to giant flux creep and vortex glass models were discussed.

Keywords MPMG method · Y_2O_3 layer · Activation energy · Pinning mechanism · Irreversibility field · Vortex glass · Vortex liquid · Giant flux creep

1 Introduction

Melt process has been accepted as a suitable method for the fabrication of large single-crystal YBCO high-temperature superconductors (HTSs) having good flux pinning and magnetic properties [1].

Since the melt–powder–melt–growth (MPMG) process is based on the reaction: Y_2BaCuO_5 (211) + L($3BaCuO_2$ + $2CuO$) → $YBa_2Cu_3O_{7-x}$(123), it is possible to make the 211 remain in the final structure by changing the starting composition toward the 211-rich regions. When the distribution of 211 is not uniform, the final structure becomes inhomogeneous and results in weak connectivity of the superconducting phase, which leads to lower critical current density (J_c). In order to promote the growth of the superconducting phase, the 211 particles must be dispersed uniformly in the liquid [2]. Since the 211-phase nucleates from Y_2O_3, it is possible to control the distribution of the 211 phase if the distribution of Y_2O_3 is controlled [3]. The 211 particles act like flux pinning centres after the fabrication process. Furthermore, it was observed that the Y_2O_3 buffer layer on crucible also prevents the liquid to spread on the furnace plate [4] and the contamination from Al_2O_3 crucible to the sample during the crystal growth of bulk YBCO.

To understand the complex pinning behaviour in high-temperature superconductors, for simplicity, we studied the effective activation energy (U) of the flux pinning dependency on the magnetic field and temperature. One accepted method for probing this dependence is to measure the resistive transition in various applied magnetic fields and temperature. It is commonly suggested that the resistivity of the high-temperature superconductors in the region of low resistivity can be described as the Arrhenius relationship [5].

✉ Sedat Kurnaz
sedatkurnaz@windowslive.com

[1] Department of Physics, Karadeniz Technical University, 61080 Trabzon, Turkey

[2] Vocational School of Health Services, Artvin Çoruh University, 08000 Artvin, Turkey

Two main theoretical lines are used for the interpretation of the irreversibility line (IL), one of which is that the vortices are thermally activated. In this case, the reversible behaviour occurs when the flux creep effects become dominant. The other line of reasoning suggests that associated with T_{irr}, a phase transition occurs [6].

Three different phases of the vortex matter were observed in YBCO single crystals: an almost perfect vortex lattice, a disordered vortex solid (or vortex glass) and vortex liquid. This rather complex phase diagram was simplified for superconductors with strong pinning in which only the vortex glass and vortex liquid were found. These both phases are separated by the irreversibility field, $H_{irr}(T)$, for the glass phase. Irreversibility field, $H_{irr}(T)$, is the highest magnetic field for applications of high-T_c superconductors [7].

In our previous works, the effects of the Y_2O_3 layer on the melt growth process were investigated and the effects on mechanical and magnetic properties were described [8–10].

In this study, YBCO samples were grown on non-layer and Y_2O_3 layers. We are interested in the effect of not using the Y_2O_3 layer and using the powder or pellet Y_2O_3 layer. Based on the Arrhenius equation, a method to calculate the activation energy, $U(T, H)$, from the resistance transition is described. The power law relationship for U with H can be determined as follows: $U(T) \propto H^{-\alpha}$, where α is the fitting parameter. Also, irreversibility lines are described from the equation $H_{irr} \sim (1 - T_{irr}(H) / T_{irr}(0))^n$. According to n values, giant flux creep (GFC) and vortex glass models are analysed in the context of thermal activation and using the Y_2O_3 layer.

2 Experimental Details

YBCO samples which are named Y1, Y2 and Y3 containing high-purity powders of Y_2O_3, $BaCO_3$ and CuO were fabricated in 1:2:3 stoichiometric ratio by the MPMG method. The details of the precursor preparation were described elsewhere [10]. The Y1 sample was placed into a platinum crucible without Y_2O_3, the Y2 sample was located on Al_2O_3 crucible with a freely poured Y_2O_3 powder and the Y3 sample was located on Al_2O_3 crucible with a 1-mm-thick buffer layer of Y_2O_3. Schematic diagram of the thermal process of these samples for crystal growth state is given in Fig. 1. Finally, the samples were annealed at 500 °C for 24 h in flowing oxygen and then cooled to room temperature at a rate of 1 °C/min in oxygen.

Magnetoresistivity measurements were performed by a standard four-point method at temperatures between 40 and 100 K with a heating rate of 4 K/min using a Quantum Design Physical Properties Measurement System (PPMS) under various constant magnetic fields parallel to the c-axis such as 0, 1, 2, 3, 4 and 5 T in the zero-field cooling (ZFC) regime.

3 Results and Discussion

3.1 Magnetoresistivity Measurements

Figure 2 shows the magnetoresistivity results of Y1, Y2 and Y3 samples. When these three samples were observed with naked eyes, the grain size of Y3 (with a 1-mm-thick buffer layer of Y_2O_3) sample was approximately 8 mm.

The superconducting transition curves measured for all samples at 0 T magnetic fields were extremely sharp. The sharpness of the transition is proportional to the degree of interconnectivity of grains. Besides, the superconducting transition temperatures skipped lower temperature with an increasing magnetic field as listed in Table 1.

Y1 (without Y_2O_3) has a maximum transition temperature (94.5 K) at a 0 T magnetic field, among these superconductors (Table 1). The width (ΔT) of superconducting transition temperatures of the Y1 (without Y_2O_3), Y2 (with a freely poured Y_2O_3 powder) and Y3 (with a

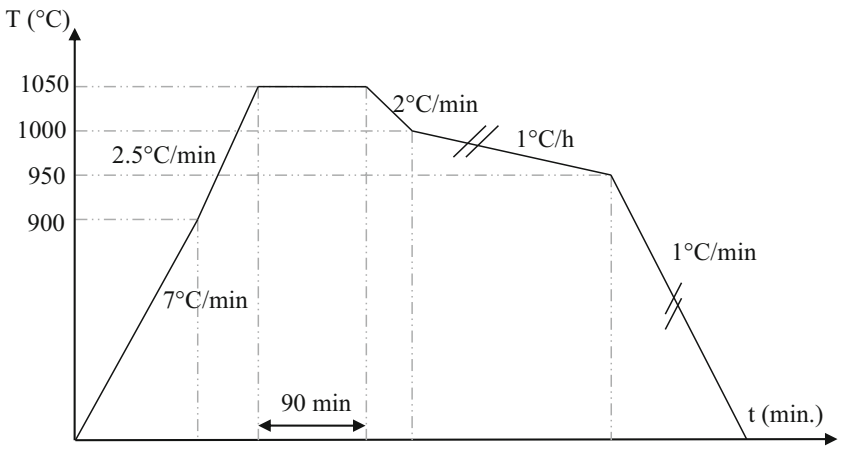

Fig. 1 Schematic diagram of the thermal process for YBCO samples at 1050 °C

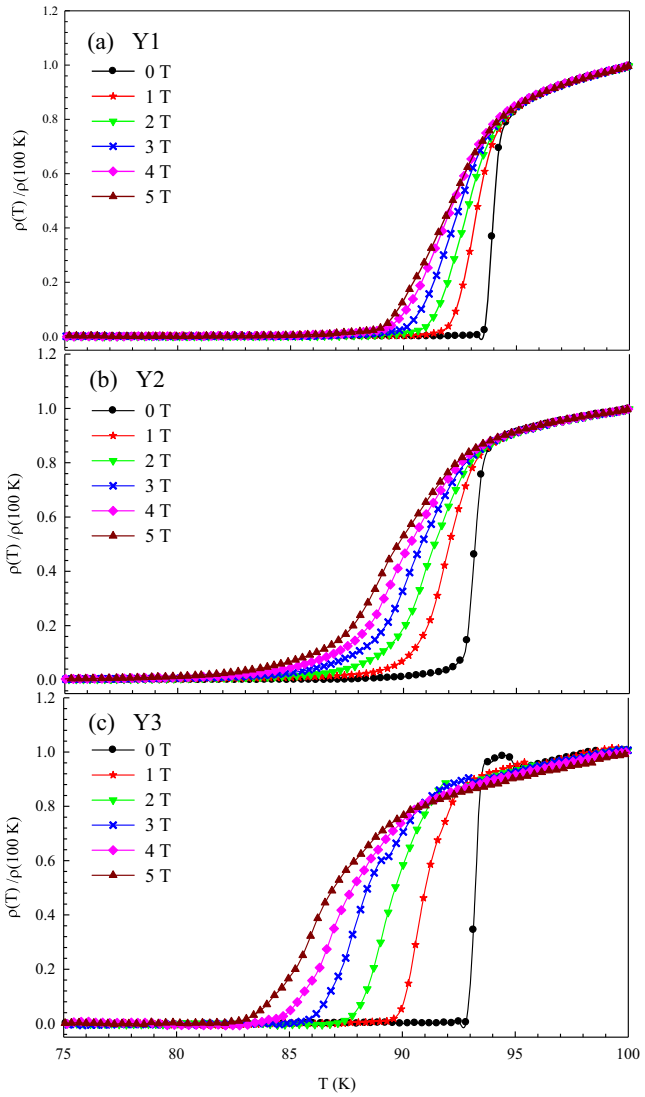

Fig. 2 The temperature dependence of normalised resistance for the **a** Y1 (without Y_2O_3), **b** Y2 (with a freely poured Y_2O_3 powder) [9] and **c** Y3 (with a 1-mm-thick buffer layer of Y_2O_3) [9] samples at different applied fields

1-mm-thick buffer layer of Y_2O_3) samples in a 5 T magnetic field appears to be nearly 5, 9 and 8 K, respectively. It is observed that the magnetoresistance of samples is resistant to the magnetic field. The weak links of the grain boundaries firstly returned to normal state by the applied magnetic field. Then, the entering magnetic field into grain is disrupted by the superconductivity. Due to the smallest width of superconducting transition temperature in the Y1 sample, this process is moving more slowly. So, the Y1 sample produced without the using of the Y_2O_3 layer is resistant to magnetic field. Moreover, the large ΔT values imply very sluggish oxygen diffusion into the large-sized single Y123 grains in spite of the presence of the Y211/Y123 interfaces [11].

Secondary 211 phase was formed by the rapid cooling process; however, it is known as an effective pinning centre, due to the expanding of the ΔT range and reducing resistance to magnetic field, not served as the effective pinning centre. When considering the peritectic reaction (Y_2O_3 + L(BaO + CuO) → Y_2BaCuO_5), some Y_2O_3 particles from the layer do participate in the reaction from the layer distributed throughout the sample, distorting the nature of pinning centres, which contributed to the reduction in the value of the pinning force. Moreover, the interaction between grains was observed that is further weakened. So, the 211 particles grow to a large size and are distributed non-uniformly, which will result in the weak connectivity of the superconducting phase [3].

Consequently, using the powder or pellet Y_2O_3 layer during the fabrication process affects negatively the resistivity properties of the samples.

3.1.1 Activation Energy

In the Anderson theory, the magnetoresistance caused the movement of vortices defined as [12]

$$\rho\left(B,T\right)=\rho_0\exp\left[-U\left(B,T\right)/k_{\mathrm{B}}T\right] \quad (1)$$

Table 1 The values of critical transition temperature for the Y1 (without Y_2O_3), Y2 (with a freely poured Y_2O_3 powder) [9] and Y3 (with a 1-mm-thick buffer layer of Y_2O_3) [9] samples at different applied fields

	0 T	1 T	2 T	3 T	4 T	5 T
Y1						
$T_{c,onset}$ (K)	94.54	94.22	94.17	94.02	93.96	93.80
$T_{c,offset}$ (K)	93.59	91.67	90.64	89.82	88.82	88.91
ΔT (K)	0.95	2.55	3.53	4.20	5.14	4.89
Y2						
$T_{c,onset}$ (K)	93.77	93.37	93.28	93.10	92.92	92.60
$T_{c,offset}$ (K)	91.59	88.66	86.87	85.82	84.66	83.66
ΔT (K)	2.18	5.11	6.41	7.28	8.26	8.94
Y3						
$T_{c,onset}$ (K)	93.45	93.04	91.62	91.41	91.08	90.70
$T_{c,offset}$ (K)	92.92	89.74	87.50	85.87	83.62	82.78
ΔT (K)	0.53	3.30	4.12	5.54	7.46	7.92

where ρ_0 is the normal resistivity, $U(B,T)$ is the flux pinning energy or activation energy for flux creep that depends on the temperature and magnetic field and k_B is the Boltzmann constant. For the case of classical flux creep [13], where $U >> k_B T$, the activation energy should not depend on temperature and the resistivity behaves as

$$\rho \approx \exp\left(-U/k_B T\right) \tag{2}$$

Figure 3 shows such a plot processed for the Y1, Y2 and Y3 samples. It is seen that the superconducting transition curve is fairly vertical and sharp at a 0 T magnetic field. As the applied magnetic field increases, the transition width expands. With the decline in slope of ln $\rho(T)$ versus $1/T$, the activation energy will decrease. The activation energy (U) values can be directly deduced from the slope of the plot of ln $\rho(T)$ versus $1/T$ in Fig. 4 and are depicted in Table 2.

The activation energy value of Y1 (without Y_2O_3) is calculated to be 2.547 eV (maximum value) whereas that of Y2 (with a freely poured Y_2O_3 powder) is found to be 1.334 eV (minimum value) at a 0 T magnetic field. When a 5 T magnetic field is applied to the samples, the activation energy value is obtained as 0.442 and 0.243 eV for Y1 and Y2, respectively. As seen from Fig. 4, decreasing of the activation energy depending on the increasing magnetic field causes vortex motion easily [14]. Moreover, using the powder or buffer Y_2O_3 layer reduces the activation energy value. As a result, it can be said that using the Y_2O_3 layer does not improve the superconducting properties of the pinning centres.

The activation energy values of the sample Y3 (with a 1-mm-thick buffer layer of Y_2O_3) are higher than those of the Y2 sample (with a freely poured Y_2O_3 powder). The reason for this is thought to come from using the buffer Y_2O_3 layer. A 1-mm-thick Y_2O_3 layer for the Y3 sample was prepared, applying 3 ton/cm^2. In this case, during the manufacturing process of the sample Y3 at the temperature of 1500 °C, Y_2O_3 contributes less to the 211 peritectic reaction than the sample Y2. The compressed Y_2O_3 particles to participate in the 211 peritectic reaction are more difficult than the powder Y_2O_3 particles. As a result, Y_2O_3 particles in the layer seem to decrease the activation energy value.

The activation energies extracted from the resistivity measurement in applied fields show a power law or logarithmic dependence on the field.

$$U \propto H^{-\alpha} \quad \text{or} \quad U \propto \ln H \tag{3}$$

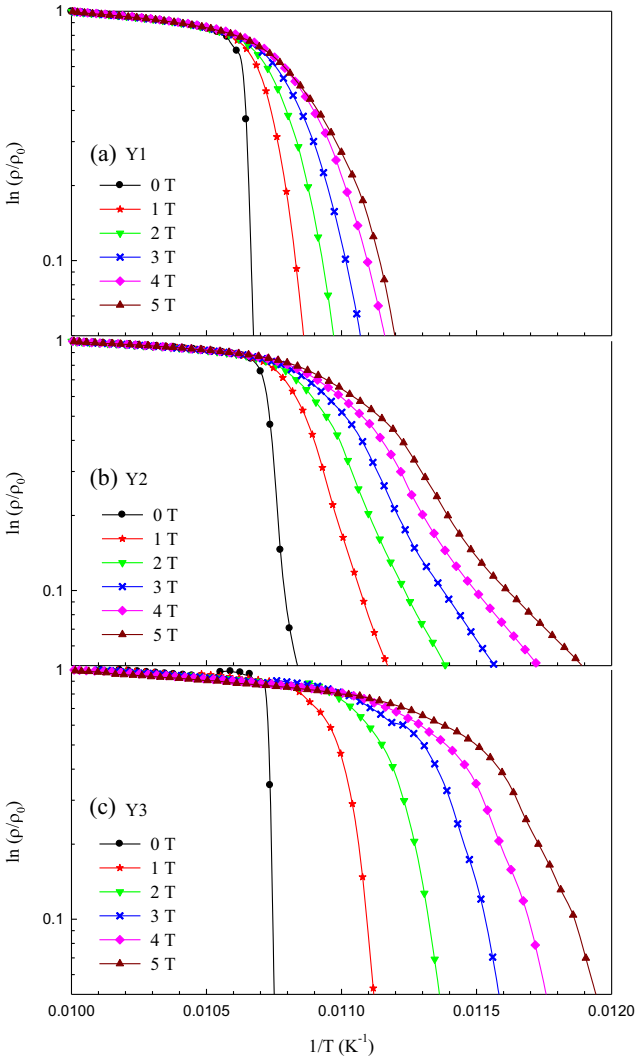

Fig. 3 ln ρ/ρ_0 versus $1/T$ graphs of the **a** Y1 (without Y_2O_3), **b** Y2 (with a freely poured Y_2O_3 powder) and **c** Y3 (with a 1-mm-thick buffer layer of Y_2O_3) samples (the activation energies of the samples are determined from the slopes of the linear parts of the low resistivity region)

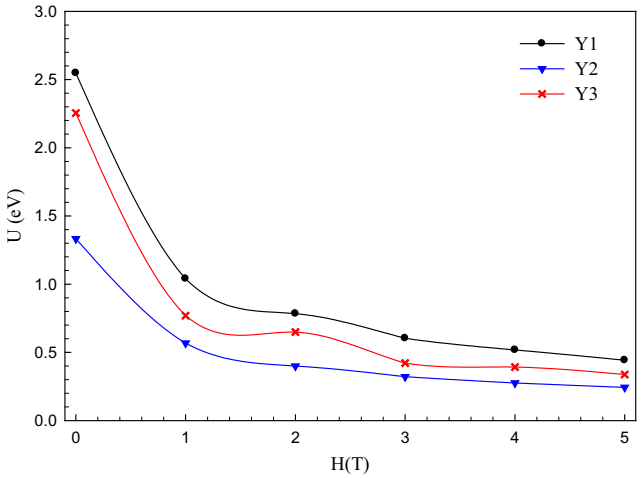

Fig. 4 The change of the activation energy values (U) of the samples with the applied magnetic field up to 5 T

Table 2 Activation energy and α values of the Y1 (without Y_2O_3), Y2 (with a freely poured Y_2O_3 powder) and Y3 (with a 1-mm-thick buffer layer of Y_2O_3) samples

	Activation energy (eV)						α
	0 T	1 T	2 T	3 T	4 T	5 T	
Y1	2.547	1.040	0.784	0.604	0.518	0.442	0.531
Y2	1.334	0.568	0.400	0.322	0.276	0.243	0.536
Y3	2.255	0.770	0.649	0.421	0.393	0.338	0.526

A ln H dependence of the activation energy $U(H)$ is often observed in superconductors. A universal viewpoint is that the planar defects are responsible for $U(H) \propto H^{-1/2}$, while the point defects are responsible for $U(H) \propto H^{-1}$ [15]. The planar defects occur whenever there is a discontinuity in the structure, for instance the grain boundaries, the interface of two surfaces, the stacking faults and the twin boundaries. The point defects occur in the case of pinholes, oxygen deficiency and small-phase particles [5].

When the data obtained from the measurements are fitted to (3) in Fig. 5, the α values are found to be 0.531, 0.536 and 0.526 for Y1, Y2 and Y3 samples, respectively. $\alpha \approx 0.5$ implies that the thermally activated dissipativity is directly associated with the planar defect pinning mechanism. The irregular nature of the planar defects is an indication of the local variations in the Y_2BaCuO_5 [16]. Additionally, we consider that some Y_2O_3 particles which do not enter the peritectic reaction, because of having excess Y_2O_3 particles, form point defects in the sample.

So, we think that using the powder or buffer Y_2O_3 layer increases the planar and point defects and, in addition, disrupts the crystal structure characteristics.

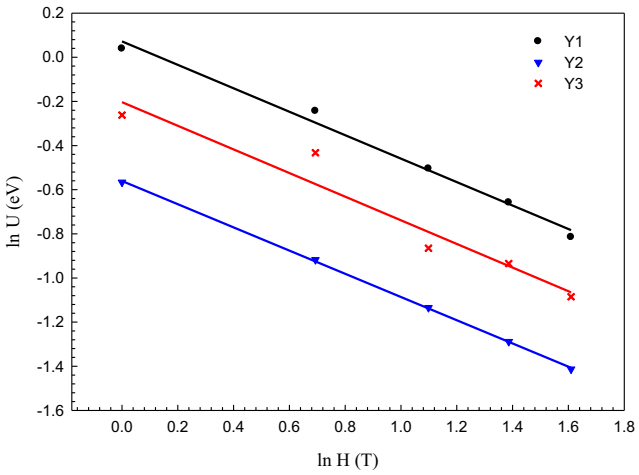

Fig. 5 Dependence of activation energy on magnetic field in logarithmic scale

3.1.2 Irreversibility Line from Magnetoresistivity Measurements

Vortex dynamics in superconductors give information about the motion of vortices as influenced by different factors (interactions, defects, etc.) [17], and the behaviours of vortex dynamics affected defects, doping, thermal fluctuations, Lorentz force, magnetic field and temperature. It is related to important quantities like the IL. The IL in the H–T plane separates the reversible (or flux flow) and irreversible (or flux pinned) regions.

IL consists of irreversibility field (H_{irr}) and irreversibility temperature (T_{irr}). $T_{irr} < T < T_{c,onset}$ and $H_{irr} < H < H_{c2}$ are defined as above the IL or reversible region where the effects of the pinning energy are negligible [18]. Above the IL, the vortices have enough energy and they can move freely [6] when the pinning force is dominated by the Lorentz force and thermal effect. Finite resistance values with the movement of the vortex will appear. When vortex pinning increases, the energy loss resulting from the vortex motion is reduced and the critical current density is increased. At the same time, permanent magnetisation increases. Due to trapped magnetic flux, the magnetisation behaviour between $T < T_{irr}$ and $H < H_{irr}$ is defined as below the IL or irreversible region. Below the IL, the Lorentz force and thermal effect on mobilising vortex movement is dominated by the pinning force. $T > T_{c,onset}$ or $H > H_{c2}$ is defined to be normal state. If $T > T_{c,onset}$ or $H > H_{c2}$, the superconductor will no longer show superconducting properties because of the extreme mobility vortex and interaction with each other.

The (GFC) model was proposed by Yeshurun and Malozemoff [19], and the proposed model was based on the flux creep model by Anderson and Kim [20]. The GFC phenomenon was observed in HTS, particularly in the yttrium-based materials, because of the relatively low pinning energies and the higher critical temperatures. The GFC apparently affects the flux dynamics, which relates to both flux pinning and thermal activation, and influences the properties of HTS [21]. According to the GFC model,

owing to the Lorentz force, the vortex begins to interact forming a triangular vortex lattice leading to dissipation and thermal fluctuations in the matrix. The thermal fluctuations are enhanced further due to larger anisotropy and crystal imperfection such as local defects, dislocations, twins and stacking faults. The Lorentz forces induce a flux motion by energy dissipation [22].

Fisher [23], considering lattice defects in the high-T_c oxide superconductor, suggested a vortex glass or vortex solid model. The vortex glass model is used to signify the destruction of long-range translational order in the Abrikosov lattice due to flux pinning by the underlying disorder in the superconducting material. The IL is shown to be a sharp boundary across a thermodynamic phase transition between the disordered vortex solid (or vortex glass) and the vortex liquid where thermally activated flux flow is possible [24]. In the mixed state of type II superconductors, if a superconductor has no impurities and lattice defects, vortices form properly sequenced like Abrikosov lattice. If the superconductor has impurities and lattice regions, these regions will attract vortices. Due to the fact that these regions are in place in random structure, they will cause the formation of crystals by disrupting the regular vortex lattice. It will cause the vortex glass lattice. At low temperature, the vortex has minimal energy. Besides, the repulsive interaction between vortices and pinning centres causes us to ignore the thermal fluctuations. When temperature begins to increase, vortices will gain heat energy and start to vibrate around their equilibrium position. So, the thermal fluctuation will become dominant. When temperature reaches a sufficient level ($T = T_{irr}$), vortex glass lattice that is disordered will melt. As a result, vortex liquid lattice will occur. IL gives information about a phase of vortices. This phase transition temperature (T_{irr}) and linear and non-linear resistance value will occur.

The H_{irr} and H_{c2} are estimated from the resistivity versus the applied magnetic field curves. As it well known from the literature [25], at various magnetic fields, the H_{irr} and H_{c2} are defined as the fields where the temperature-dependent resistance is

$$\rho\ (H_{irr}, T) = 0.1\ \rho_n \tag{4}$$

$$\rho\ (H_{c2}, T) = 0.9\ \rho_n \tag{5}$$

where ρ_n indicates the normal-state resistance of the samples at $T_{c,onset}$. Finding H_{irr}–T (T_{irr}) and H_{c2}–T from (4) and (5) was drawn in the field–temperature plane.

The irreversibility line is drawn using (6) [26]

$$H_{irr} = H_0 \left(1 - \frac{T_{irr}(H)}{T_{irr}(0)}\right)^n \tag{6}$$

$T_{irr}(0)$ is the irreversibility temperature at zero applied field. $T_{irr}(H)$ is the irreversibility field at different applied fields. The fitting parameters H_0 and n are calculated according to the equation $y = ax^b$. According to the H_0 and n found, new H_{irr} values are obtained. Looking at these values, a fitting curve is drawn using (6).

It has values between 1.5 and 5.5 and is related to the degree of anisotropy in the system [27] for samples fabricated using a seed crystal. In the case of YBCO, for $n \approx 1.5$, IL is dominated by the GFC and vortex glass models [19, 23].

Figure 6 shows the vortex glass, the irreversibility line, the reversible region (or vortex liquid) and normal state

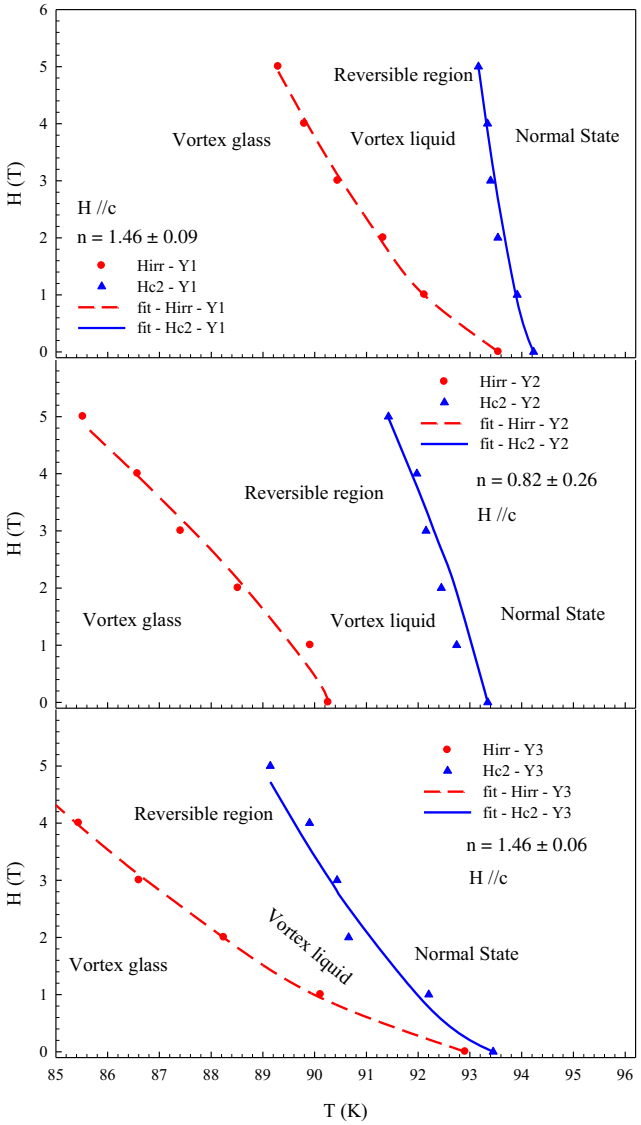

Fig. 6 $H_{irr,}$ H_{c2}, irreversibility line, reversible region, vortex glass, vortex liquid and normal state from magnetoresistivity measurements for the **a** Y1 (without Y_2O_3), **b** Y2 (with a freely poured Y_2O_3 powder) and **c** Y3 (with a 1-mm-thick buffer layer of Y_2O_3) samples

Table 3 H_{irr}, H_{c2} and T values from magnetoresistivity measurement for the Y1 (without Y_2O_3), Y2 (with a freely poured Y_2O_3 powder) and Y3 (with a 1-mm-thick buffer layer of Y_2O_3) samples

	0 T	1 T	2 T	3 T	4 T	5 T
Y1						
T (K), $\mu_0 H_{irr}$ (T)	93.65	92.12	91.32	90.45	89.80	89.30
T (K), $\mu_0 H_{c2}$ (T)	94.23	93.91	93.35	93.40	93.34	93.16
Y2						
T (K), $\mu_0 H_{irr}$ (T)	90.26	89.92	88.52	87.41	86.58	85.53
T (K), $\mu_0 H_{c2}$ (T)	93.35	92.74	92.45	92.15	91.97	91.43
Y3						
T (K), $\mu_0 H_{irr}$ (T)	92.91	90.12	88.25	86.61	85.44	84.17
T (K), $\mu_0 H_{c2}$ (T)	93.45	92.20	90.66	90.43	89.90	89.14

from magnetoresistivity measured for the Y1, Y2 and Y3 samples, and the temperatures for the H_{irr} and H_{c2} are listed in Table 3.

The wider reversible region is not suitable for superconducting applications. Because of the vortex mobility and the transition from superconducting state to normal state, resistance will occur. In Fig. 6, the reversible region of the Y1 sample (without Y_2O_3) is narrower than the reversible region of Y2 and Y3 samples.

In Y2 and Y3 samples, Y_2O_3 particles from the layer do not act like the flux pinning centres. Therefore, it is seen that the reversible region expands even more. It does not show a homogeneous distribution of Y_2O_3 particles which cause planar defects in structure. In some areas, more intensive distribution and the thermal effect from this distribution are thought to be dominant and this dominance will lead to a decrease of the pinning force.

When n parameters are evaluated for all samples (Table 4), as a result, the Y1 (without Y_2O_3) and Y3 (with a 1-mm-thick buffer layer of Y_2O_3) [20] samples seem to exhibit behaviour by GFC and vortex glass models. In addition to having the same n exponential parameters and due to having narrower reversible region, it is seen that the Y1 sample has better properties.

Table 4 Power law exponent (n) and the parameter H_0 and T_{irr} values from fitting of the Y1 (without Y_2O_3), Y2 (with a freely poured Y_2O_3 powder) and Y3 (with a 1-mm-thick buffer layer of Y_2O_3) samples to the flux creep power law generated from the data given in Fig. 6

	$\mu_0 H_0$(T)	n	T_{irr}(K)
Y1	458.57	1.46 ± 0.09	93.65
Y2	54.15	0.82 ± 0.26	90.26
Y3	157.01	1.46 ± 0.06	92.82

4 Conclusion

In the magnetoresistivity measurements,

1. Using the Y_2O_3 layer after the fabrication process affects negatively the resistivity properties of the samples.
2. Using the powder or pellet Y_2O_3 layer seems to decrease the activation energy value. $\alpha \approx 0.5$ can be attributed to planar defects. Furthermore, due to excess Y_2O_3 particles, point defects can be seen in the sample. When both defects are considered, it is seen that the planar defects are more dominant than the point defects.
3. According to $n \approx 1.5$ parameter, the Y1 (without Y_2O_3) and Y3 (with a 1-mm-thick buffer layer of Y_2O_3) samples exhibit behaviour by GFC and vortex glass model.

The effect of using different Y_2O_3 layers was investigated, and it was seen that the Y_2O_3 layer was not served as flux pinning centres and disrupted the superconductivity at 1050 °C.

Funding Information This study was supported by the Turkish Scientific and Research Council (TUBITAK) research grant (TBAG-107T751) and Karadeniz Technical University research grant (BAP-2008.111.001.8)

References

1. Ullrich, M., Walter, H., Leenders, A., Freyhardt, H.C.: Batch production of high-quality-customized-shaped-monolithic HTSC. Phys. C **311**, 86 (1999)
2. Murakami, M., Oyama, T., Fujimoto, H., Gotoh, S., Yamaguchi, K., Shiohara, Y., Koshizuaka, N., Tanaka, S.: Melt processing of bulk high-T_c superconductors and their application. IEEE Trans. Mag **27**, 1479 (1991)

3. Murakami, M.: Processing of bulk YBaCuO. Supercond. Sci. Technol. **5**, 185 (1992)
4. Chaud, X., Isfort, D., Beaugnon, E., Tournier, R.: Isothermal growth of large $YBa_2Cu_3O_{7-x}$ single domains up to 93 mm. Phys. C **2413**, 341 (2000)
5. Zou, X.W., Wang, Z.H., Chen, J.L., Zhang, H.: Effective activation energy U(T, H) in Na-doped MTG-YBCO crystals. Phys. C **31**, 356 (2001)
6. Parra Vargas, C.A., Pimentel, J.L.Jr., Pureur, P., Landinez Tellez, D.A., Roa-Rojas, J.: Magnetization fluctuation analysis and superconducting parameters of $La_{0.5}RE_{0.5}BaCaCu_3O_{7-\delta}$ (RE = Y, Sm, Gd, Dy, Ho, Yb) superconductor. Phys. B **407**, 3128 (2012)
7. Skourski, Y., Fuchs, G., Kerschl, P., Kozlov, N., Eckert, D., Nenkov, K., Müller, K.H.: Magnetization and magneto-resistance measurements of bulk $YBa_2Cu_3O_{7-x}$ in pulsed magnetic fields up to 50 T. Phys. B **325**, 325 (2004)
8. Aydıner, A., Çakır, B., Başoğlu, M., Yanmaz, E.: The effect of excess Y_2O_3 addition on the mechanical properties of melt-processed YBCO superconductor. J. Supercond. Nov. Magn. **23**, 1493 (2010)
9. Aydıner, A., Çakır, B., Seki, H., Başoğlu, M., Wongsatanawarid, A., Murakami, M., Yanmaz, E.: The effect of Y_2O_3 buffer layer on the magnetic properties of melt-processed YBCO superconductor. J. Supercond. Nov. Magn. **24**, 1397 (2011)
10. Çakır, B., Aydıner, A.: Preparation and properties of MPMG YBCO bulk with Y_2O_3 layer. J. Supercond. Nov. Magn. **24**, 1577 (2011)
11. Jun, B.H., Jung, S.A., Park, S.D., Park, B.J., Han, Y.H., Kim, C.J.: Effects of Y_2O_3 additions on the oxygen diffusion in top-seeded melt growth processed $YBa_2Cu_3O_{7-y}$ superconductors. Phys. C **471**, 876 (2011)
12. Anderson, P.W.: Theory of flux creep in hard superconductors. Phys. Rev. Lett. **9**, 309 (1962)
13. Balaev, D.A., Dubrovskiy, A.A., Popkov, S.I., Shaykhutdinov, K.A., Petrov, M.I.: Magnetic field dependence of intergrain pinning potential in bulk granular composites YBCO plus CuO demonstrating large magneto-resistive effect. J. Supercond. Nov. Magn. **243**, 21 (2008)
14. Nikolo, M., Goldfarb, R.B.: Flux creep and activation-energies at the grain-boundaries of Y-Ba-Cu-O superconductors. Phys. Rev. B **39**, 6615 (1989)
15. Yang, T., Wang, Z.H., Zhang, H., Fang, J., Nie, Y., Qiu, L., Ding, S.Y.: Effective activation energy and phase diagram in the Er-doping MTG-$YBa_2Cu_3O_{7-\delta}$ crystal. Phys. C **384**, 130 (2003)
16. Cloet, V., Thersleff, T., Stadel, O., Hoste, S., Holzapfel, B., Van Driessche, I.: Transmission electron microscopy analysis of a coated conductor produced by chemical deposition methods. Acta Mater. **58**, 1489 (2010)
17. Marino, A., Sanchez, H., Martinez, H.: BISCCO Thin films: superconducting phases, irreversibility line and critical current. J. Supercond. Nov. Magn. **28**, 391 (2015)
18. Pena, J.P., Martinez, D.B., Pureur, P.: Magnetic measurements and kinetic energy of the superconducting condensate in $SmBa_2Cu_3O_{7-\delta}$. Braz. J. Phys. **43**, 22 (2013)
19. Yeshurun, Y., Malozemoff, A.P.: Giant flux creep and irreversibility in an Y-Ba-Cu-O crystal—an alternative to the superconducting-glass model. Phys. Rev. Lett. **60**, 2202 (1988)
20. Anderson, P., Kim, Y.: Hard superconductivity: theory of motion of Abrikosov flux lines. Rev. of Modern Phys. **36**, 39 (1964)
21. Luo, H., Ding, S.Y., Wu, X.F., Wang, Z.H., Luo, H.M.: The numerical of influence of flux creep on AC losses in superconductors. J. of Supercond. **14**, 631 (2001)
22. Kujur, A., Behera, D.: Magneto-transport studies in (1-X)$YBa_2Cu_3O_{(7-\delta)}$+X $BaTiO_3$ superconductors. J. Magn Magn Mater **377**, 34 (2015)
23. Fisher, M.P.A.: Vortex-glass superconductivity—a possible new phase in bulk high-T_c oxides. Phys. Rev. Lett. **62**, 1415 (1989)
24. Chandra, J., Manekar, M., Sharma, V.K., Mondal, P., Tiwari, P., Roy, S.B.: Vortex matter in highly strained $Nb_{75}Zr_{25}$: analogy with viscous flow of disordered solids. J. of Low Temp. Phys. **186**, 21 (2017)
25. Kumakura, H., Kitaguchi, H., Matsumoto, A., Yamada, H.: Upper critical field, irreversibility field, and critical current density of powder-in-tube-processed MgB_2/Fe tapes. Supercond. Sci. Technol. **18**, 1042 (2005)
26. Valladares, L.D., Dominguez, A.B., Quispe, R.B., Santibanez, W.F., Aguiar, J.A., Barnes, C.H.W., Majima, Y.: The irreversibilityline and Curie-Weiss temperature of the superconductor $LaCaBaCu_{3-X}(BO_3)(_X)$ with x=0.2 and 0.3. Phys. Procedia **36**, 354 (2012)
27. Mostafa, M.F., Hassen, A., Kunkel, H.P.: Irreversibility line of an Ag-doped Hg-based superconductor. Supercond. Sci. Technol. **23**, 085010 (2010)